Geometry-dependent dynamics of two Λ-type atoms via vacuum-induced coherences

Jörg Evers, Martin Kiffner, Mihai Macovei, and Christoph H. Keitel
Max-Planck-Institut für Kernphysik, Saupfercheckweg 1, D-69117 Heidelberg, Germany
(Received 30 November 2005; published 6 February 2006)

The dynamics of a pair of atoms can significantly differ from the single-atom dynamics if the distance of the two atoms is small on a scale given by the relevant transition wavelengths. Here, we discuss two nearby three-level atoms in Λ configuration, and focus on the dependence of the optical properties on the geometry of the setup. We find that in general transitions in the two atoms can be dipole-dipole coupled by interactions via the vacuum field even if their transition dipole moments are orthogonal. We give an interpretation of this effect and show that it may crucially influence the system dynamics. In particular, for a fixed setup of driving fields and detectors, the spatial orientation of the two-atom pair decides if the system reaches a true constant steady state or if it exhibits periodic oscillations in the long-time limit. As an example observable, we study the resonance fluorescence intensity, which is either constant or is modulated periodically in the long-time limit.

DOI: 10.1103/PhysRevA.73.023804 PACS number(s): 42.50.Fx, 42.50.Lc, 42.50.Ct

I. INTRODUCTION

In collections of nearby atoms, the various particles can interact via the common vacuum radiation field in a process where a (virtual) photon emitted by one of the atoms is reabsorbed by another atom. This process gives rise to a collective quantum dynamics, which can significantly deviate from a corresponding single-particle dynamics. Apart from larger ensembles of nearby quantum objects which require a statistical treatment [1–13], also few-particle quantum systems have attained considerable interest [14–24]. These systems reveal interesting cooperative effects, but are still small enough such that the constituents can be treated individually. Subradiance and superradiance was studied, e.g., in Ref. [1–3,14], while two-atom resonance fluorescence was discussed in Ref. [15]. Other studies include frequency shifts [16], collective quantum jumps [17], two-photon resonances [18], or entanglement [19,20]. Some of these effects have been verified experimentally [21]. Further references on collective two-atom systems can be found, e.g., in Refs. [5,22]. Most of these works have focused on two-level systems, often restricted to somewhat special geometries. For example, the alignment of the transition dipole moments, the interatomic distance vectors, the laser field wave vectors, and the observation direction are often assumed fixed and parallel or perpendicular to each other.

For collective effects to occur, the distance between two particles should not significantly exceed the involved transition wavelength, which can be understood from the time-energy uncertainty relation applied to the exchanged photon. Another restriction arises from the fact that the polarization of the emitted photon must match the absorbing transition [3,4]. Thus usually this dipole-dipole interaction is thought to couple only nonorthogonal transition dipole moments. This restriction is in complete analogy to the stringent conditions for the appearance of spontaneous-emission interference in single-particle systems, which was studied intensively due to the large range of possible applications [4,25–28].

Recently, a collection of two nearby three-level systems in the *V* configuration was studied in a more general geometric setup [24], with the emphasis on vacuum-mediated couplings. Interestingly, the authors found a new type of vacuum-induced coherences, which arises from dipole-dipole coupling of transitions with *orthogonal* dipole moments. In Ref. [24], however, little physical interpretation of the effect is given, and no external driving field but the vacuum was considered.

Thus in this article, we study two nearby laser-driven three-level systems in the Λ configuration as shown in Fig. 1. We demonstrate that the vacuum-induced dipole-dipole coupling of orthogonal transition dipole moments can crucially influence the dynamics of the laser-driven system. For otherwise fixed parameters and experimental setup, the relative position of the two atoms alone can decide whether the system has a stationary steady state or not. The nonstationary steady states occur even though each of the involved atomic transitions is driven by a single laser field only. As an example observable, we discuss the total fluorescence intensity emitted by the composite system, which is either stationary or "blinks" at a characteristic frequency in the long-time limit. In the final part, we give a physical interpretation for the new coherences, and show that the coupling of orthogonal dipole moments can be explained in terms of the dipole radiation pattern.

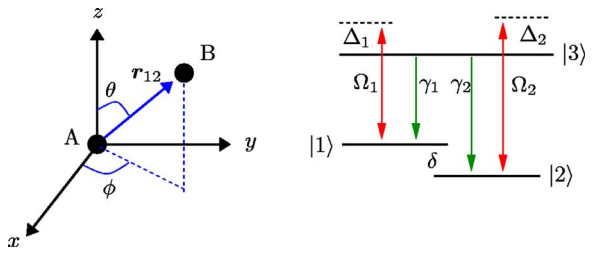

FIG. 1. (Color online) The system setup. Atom A is located in the coordinate origin, atom B at $\boldsymbol{r}_{12}$, as shown in the left part of the figure. In our coordinate system, the interatomic distance vector is parametrized by the length r_{12} and the angles θ, ϕ. Internally, both atoms (A, B) are three-level systems in Λ configuration as shown in the right subfigure. Ω_1 (Ω_2) is the Rabi frequency of the driving laser field coupling to transition $1 \leftrightarrow 3$ ($2 \leftrightarrow 3$) with detuning Δ_1 (Δ_2). The two lower states have frequency difference δ. The spontaneous decay rates are γ_1, γ_2.

Our results are of relevance for experimental realizations of collective few-level systems. If the system geometry is not fixed to one of few special cases, then additional interactions between the considered transitions lead to a nontrivial modification of the dynamics. Furthermore, unwanted couplings to additional transitions can occur via the vacuum, even if no laser field is applied to the unwanted transitions. Then, for example, a few-level approximation of the system may break down. Finally, the geometry-dependent effects provide an extended set of observables in the study of samples of nearby atoms. Potential applications include precision three-dimensional (3D) measurements of relative positions and distances of the involved particles, or the modification of the collective dynamics via a controlled change in the system geometry.

The article is organized as follows. In Sec. II, we introduce the system of interest and analytically derive the master equation governing the system and the expressions for the emitted fluorescence intensity. In the following Sec. III, we numerically solve the master equation and present our results. In Sec. IV, we provide a physical interpretation of the new coherences and explain why orthogonal transition dipoles can be coupled. Finally, Sec. V discusses and summarizes the results.

II. ANALYTICAL CONSIDERATIONS

We consider two three-level systems in Λ configuration as shown in Fig. 1. The two lower states have an energy separation δ. The two transition dipole moments of each individual atom are assumed perpendicular as, e.g., for the case of Zeeman sublevels. The dipole moments of the two atoms are aligned, e.g., by a magnetic field. We place the origin of the coordinate system at the location of the first atom $\boldsymbol{r}_1=(0,0,0)^T$; the second atom is located at $\boldsymbol{r}_2=\boldsymbol{r}_{12}=r_{12}(\sin\theta\cos\phi,\sin\theta\sin\phi,\cos\theta)^T$. Thus the interatomic distance vector is $\boldsymbol{r}_{12}$. The driving fields propagate in z direction. For simplicity, we assume real dipole moments. The dipole moment $\boldsymbol{d}_1$ of the $1\leftrightarrow 3$ transition is taken to be identical for both atoms, and aligned in the x direction. The second dipole moment $\boldsymbol{d}_2$ corresponding to the $2\leftrightarrow 3$ transition is along the y direction for both atoms. The system Hamiltonian is given by

$$H = H_a + H_f + H_{\mathrm{vac}} + H_L, \tag{1}$$

where

$$H_a = \sum_{\mu=1}^{2}\sum_{j=1}^{3} \hbar\omega_j S_{jj}^{(\mu)}, \tag{2}$$

$$H_f = \sum_{\boldsymbol{k}\lambda} \hbar\omega_{k\lambda} a_{\boldsymbol{k}\lambda}^{\dagger} a_{\boldsymbol{k}\lambda}, \tag{3}$$

$$H_{\mathrm{vac}} = -\sum_{\mu=1}^{2} [(\boldsymbol{d}_1 S_{31}^{(\mu)} + \boldsymbol{d}_2 S_{32}^{(\mu)})\boldsymbol{E}(\boldsymbol{r}_\mu) + \mathrm{H.c.}], \tag{4}$$

$$H_L = -\hbar\sum_{\mu=1}^{2} [\Omega_1(\boldsymbol{r}_\mu)e^{-i\nu_1 t}S_{31}^{(\mu)} + \Omega_2(\boldsymbol{r}_\mu)e^{-i\nu_2 t}S_{32}^{(\mu)} + \mathrm{H.c.}]. \tag{5}$$

Here, $S_{ij}^{(k)}=|i\rangle_{kk}\langle j|$ $(i\in\{1,2,3\}, j\in\{1,2\})$ is the population of state i of atom k for $i=j$, and a transition operator for atom k for $i\neq j$. $\hbar\omega_i$ is the energy of state $|i\rangle$ of each of the atoms, $\omega_{k\lambda}$ is the frequency of the vacuum field mode with creation (annihilation) operator $a_{\boldsymbol{k}\lambda}^{\dagger}$ $(a_{\boldsymbol{k}\lambda})$. $\boldsymbol{E}(\boldsymbol{r})$ is the vacuum field. The driving laser fields have frequencies ν_j, polarization unit vectors $\hat{\boldsymbol{\epsilon}}_j$ and amplitudes $\mathcal{E}_j$. The corresponding Rabi frequencies are $\Omega_j(\boldsymbol{r})=\Omega_j\exp[i\boldsymbol{k}_j\cdot\boldsymbol{r}]$, where $\Omega_j=(\boldsymbol{d}_j\cdot\hat{\boldsymbol{\epsilon}}_j)\mathcal{E}_j/\hbar$. The free energy of the atomic states is described by H_a, H_f is the free energy of the vacuum field, H_{vac} is the interaction Hamiltonian with the vacuum field modes, and H_L describes the interaction with the laser fields in rotating-wave approximation (RWA).

In a suitable interaction picture, using the RWA and the Born-Markov approximation, the system can be described by a master equation for the atomic density operator ρ given by

$$\begin{aligned}\frac{\partial\rho}{\partial t} =& -i\sum_{\mu=1}^{2}\sum_{j=1}^{2}[\Delta_j S_{jj}^{(\mu)},\rho] + i\sum_{\mu=1}^{2}\sum_{j=1}^{2}[(S_{3j}^{(\mu)}\Omega_j(\boldsymbol{r}_\mu)+\mathrm{H.c.}),\rho]\\ &-\sum_{\mu=1}^{2}\sum_{j=1}^{2}[\gamma_j(S_{33}^{(\mu)}\rho - 2S_{j3}^{(\mu)}\rho S_{3j}^{(\mu)} + \rho S_{33}^{(\mu)}) + \Gamma_j^{dd}(S_{3j}^{(\mu)}S_{j3}^{(\neg\mu)}\rho\\ &-2S_{j3}^{(\neg\mu)}\rho S_{3j}^{(\mu)} + \rho S_{3j}^{(\mu)}S_{j3}^{(\neg\mu)})] + \sum_{j=1}^{2}(i\Omega_j^{dd}[S_{3j}^{(1)}S_{j3}^{(2)},\rho]\\ &+\mathrm{H.c.}) - \sum_{\mu=1}^{2}[\Gamma_{vc}^{dd}(S_{32}^{(\mu)}S_{13}^{(\neg\mu)}\rho - 2S_{13}^{(\neg\mu)}\rho S_{32}^{(\mu)}\\ &+\rho S_{32}^{(\mu)}S_{13}^{(\neg\mu)})e^{i\Delta t} + \mathrm{H.c.}] + \sum_{\mu=1}^{2}(i\Omega_{vc}^{dd}[S_{32}^{(\mu)}S_{13}^{(\neg\mu)},\rho]e^{i\Delta t}\\ &+\mathrm{H.c.}).\end{aligned} \tag{6}$$

Here, $\neg\mu$ is 1 for $\mu=2$ and 2 for $\mu=1$, i.e., it denotes the atom other than μ. Further, $\Delta=\delta+\Delta_2-\Delta_1=\nu_2-\nu_1$, where $\delta=\omega_{12}$, $\Delta_i=\nu_i-\omega_{3i}$, and $\omega_{ij}=\omega_i-\omega_j$. Thus the residual time dependence can be traced back to the frequency difference of the two driving laser fields, even though each atomic transition is driven by a single laser field only. The first term on the right hand side of Eq. (6) contains the detunings Δ_i of the driving laser fields and is due to the chosen interaction picture. The second contribution with $\Omega_j(\boldsymbol{r}_\mu)$ contains the interaction with the driving laser fields. The term with γ_j describes the usual individual spontaneous decay on each of the transitions, where the spontaneous emission rate on transition $3\leftrightarrow j$ is given by $2\gamma_j$. The term proportional to Γ_j^{dd} contains the dipole-dipole cross decay between a dipole of one of the atoms and the corresponding parallel dipole of the other atom. The contribution with Ω_j^{dd} is the corresponding dipole-dipole energy shift. Finally, Γ_{vc}^{dd} and Ω_{vc}^{dd} are the cross coupling and the energy shift related to dipole-dipole interaction between a dipole of one of the atoms and the *perpendicular* dipole of the other atom. These are due to the pecu-

liar vacuum-coupling of transitions with perpendicular dipole moments, which do not occur in single-atom systems. The physical interpretation of these terms will be given in Sec. V. The explicit expressions for the spontaneous decay constants are

$$\gamma_i = \frac{1}{4\pi\epsilon_0}\frac{2|\boldsymbol{d}_i|^2\omega_{3i}^3}{3\hbar c^3}, \tag{7}$$

the dipole-dipole coupling constants are given by [24]

$$\Gamma_i^{dd} = \frac{1}{\hbar}[\boldsymbol{d}_i \cdot \mathrm{Im}(\overleftrightarrow{\chi}) \cdot \boldsymbol{d}_i^*], \tag{8}$$

$$\Omega_i^{dd} = \frac{1}{\hbar}[\boldsymbol{d}_i \cdot \mathrm{Re}(\overleftrightarrow{\chi}) \cdot \boldsymbol{d}_i^*], \tag{9}$$

$$\Gamma_{vc}^{dd} = \frac{1}{\hbar}[\boldsymbol{d}_2 \cdot \mathrm{Im}(\overleftrightarrow{\chi}) \cdot \boldsymbol{d}_1^*], \tag{10}$$

$$\Omega_{vc}^{dd} = \frac{1}{\hbar}[\boldsymbol{d}_2 \cdot \mathrm{Re}(\overleftrightarrow{\chi}) \cdot \boldsymbol{d}_1^*]. \tag{11}$$

Here, Re and Im denote the real and imaginary part, and the components of the tensor $\overleftrightarrow{\chi}$ are

$$\chi_{\mu\nu}(\boldsymbol{r}_1,\boldsymbol{r}_2) = \frac{1}{4\pi\epsilon_0}\left[\delta_{\mu\nu}\left(\frac{k_0^2}{r_{12}} + \frac{ik_0}{r_{12}^2} - \frac{1}{r_{12}^3}\right) - \frac{(\boldsymbol{r}_{12})_\mu(\boldsymbol{r}_{12})_\nu}{r_{12}^2} \times\left(\frac{k_0^2}{r_{12}} + \frac{3ik_0}{r_{12}^2} - \frac{3}{r_{12}^3}\right)\right]e^{ik_0 r_{12}}, \tag{12}$$

where $\delta_{\mu\nu}$ is the Kronecker delta symbol. Note that we have approximated $\omega_{31} \approx \omega_{32} \approx \omega_0$ in evaluating the dipole-dipole coupling constants.

In the following, we will investigate the fluorescence intensity emitted by the pair of atoms and measured by a detector at point $\boldsymbol{R} = R\hat{\boldsymbol{R}}$. It is proportional to the normally ordered correlation function

$$I = \langle :\boldsymbol{E}^{(-)}(\boldsymbol{R},t)\boldsymbol{E}^{(+)}(\boldsymbol{R},t):\rangle, \tag{13}$$

where $\boldsymbol{E}(\boldsymbol{x},t) = \boldsymbol{E}^{(-)}(\boldsymbol{x},t) + \boldsymbol{E}^{(+)}(\boldsymbol{x},t)$ and $\boldsymbol{E}^{(\mp)}(\boldsymbol{x},t)$ are the positive and negative frequency parts of the vacuum field with $[\boldsymbol{E}^{(+)}(\boldsymbol{x},t)]^\dagger = \boldsymbol{E}^{(-)}(\boldsymbol{x},t)$. We write the field in the Schrödinger picture as

$$\boldsymbol{E}^{(+)}(\boldsymbol{x},t) = i\sum_{\boldsymbol{k}\lambda} \boldsymbol{u}_{\boldsymbol{k}\lambda}(\boldsymbol{x})a_{\boldsymbol{k}\lambda} \tag{14}$$

with

$$\boldsymbol{u}_{\boldsymbol{k}\lambda}(\boldsymbol{x}) = \sqrt{\frac{\hbar\omega_k}{2\epsilon_0 V}}\hat{\boldsymbol{\epsilon}}_{\boldsymbol{k}\lambda}e^{i\boldsymbol{k}\cdot\boldsymbol{x}}. \tag{15}$$

The Heisenberg equation of motion for the annihilation operator $a_{\boldsymbol{k}\lambda}$ is given by

$$\frac{d}{dt}a_{\boldsymbol{k}\lambda} = \frac{1}{i\hbar}[a_{\boldsymbol{k}\lambda},H] = -i\omega_k a_{\boldsymbol{k}\lambda} + \frac{1}{\hbar}\sum_{\mu=1}^{2}(\boldsymbol{d}_1 S_{31}^{(\mu)} + \boldsymbol{d}_2 S_{32}^{(\mu)})\boldsymbol{u}_{\boldsymbol{k}\lambda}(\boldsymbol{r}_\mu)^* + \frac{1}{\hbar}\sum_{\mu=1}^{2}(\boldsymbol{d}_1^* S_{13}^{(\mu)} + \boldsymbol{d}_2^* S_{23}^{(\mu)})\boldsymbol{u}_{\boldsymbol{k}\lambda}(\boldsymbol{r}_\mu)^*. \tag{16}$$

By formally integrating the expression for $a_{\boldsymbol{k}\lambda}$, the electric field operator in the far field limit $R \gg r_{12}$ can be derived. It can be split up in a source part and a free part, where the latter can be neglected if the detector is placed outside of the laser field. The source part $\boldsymbol{E}_S^{(+)}(\boldsymbol{x},t)$ of the electric field operator evaluates to

$$\boldsymbol{E}_S^{(+)}(\boldsymbol{x},t) = -\sum_{\mu=1}^{2}\sum_{j=1}^{2}\frac{\omega_{3j}^2}{4\pi\epsilon_0 c^2}\frac{\hat{\boldsymbol{R}}\times(\hat{\boldsymbol{R}}\times\boldsymbol{d}_j)}{R}\cdot S_{j3}^{(\mu)}(t)e^{-ik_j\hat{\boldsymbol{R}}\cdot\boldsymbol{r}_\mu}. \tag{17}$$

Here, we have ignored retardation effects [29]. Then the intensity can be written as

$$I = \sum_{j=1}^{2}\left(w_j^2\sum_{\mu,\nu=1}^{2}\langle S_{3j}^{(\mu)}S_{j3}^{(\nu)}\rangle e^{ik_j\hat{\boldsymbol{R}}\cdot\boldsymbol{r}_{\mu\nu}}\right) - \bar{w}_1\bar{w}_2\sum_{\mu,\nu=1}^{2}\langle S_{31}^{(\mu)}S_{23}^{(\nu)}\rangle e^{i\hat{\boldsymbol{R}}\cdot(k_1\boldsymbol{r}_\mu - k_2\boldsymbol{r}_\nu)} - \bar{w}_1\bar{w}_2\sum_{\mu,\nu=1}^{2}\langle S_{32}^{(\mu)}S_{13}^{(\nu)}\rangle e^{i\hat{\boldsymbol{R}}\cdot(k_2\boldsymbol{r}_\mu - k_1\boldsymbol{r}_\nu)}, \tag{18}$$

with prefactors $w_j = \alpha_j \sin\varphi_j$ and $\bar{w}_j = \alpha_j\cos\varphi_j$, where $\alpha_j = (\omega_{3j}^2 d_j)/(4\pi\epsilon_0 c^2 R)$. The angle between the observation direction $\hat{\boldsymbol{R}}$ and the dipole moment $\boldsymbol{d}_j$ is φ_j. Note that the expectation values in Eq. (18) should be evaluated with respect to the Schrödinger picture density matrix of the system. The first line of Eq. (18) contains the individual emission of each of the two transitions $1 \leftrightarrow 3$ and $2 \leftrightarrow 3$ from both of the atoms. The other two lines are cross terms which contain contributions of both transitions. In the following, we assume our detector to be placed on the y axis, i.e., $\hat{\boldsymbol{R}} = (0,1,0)^T$. Then $\sin\varphi_2 = 0 = \cos\varphi_1$, and the intensity reduces to

$$I_y = w_1^2\sum_{\mu,\nu=1}^{2}\langle S_{31}^{(\mu)}S_{13}^{(\nu)}\rangle e^{ik_1\hat{\boldsymbol{R}}\cdot\boldsymbol{r}_{\mu\nu}}. \tag{19}$$

III. NUMERICAL RESULTS

In this section, we numerically integrate the density matrix Eq. (6) for the configuration outlined in the previous section. Thus the first atom is at the coordinate origin, the second atom is at position $\boldsymbol{r}_{12}$, the laser fields propagate in z direction, and the detector is placed in the y direction. We fix all parameters except for the angles θ and ϕ which determine the 3D orientation of the two-atom system. As initial conditions, we choose both atoms to be in the excited state $|3\rangle$.

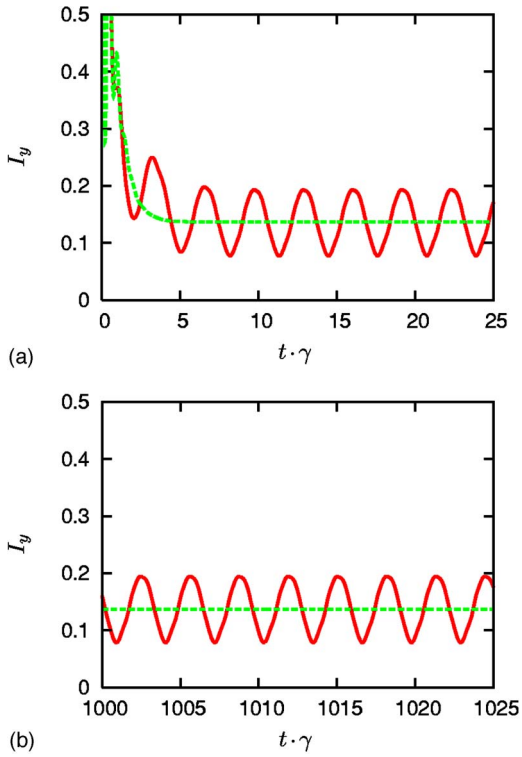

FIG. 2. (Color online) The time-dependent fluorescence intensity I_y. The parameters chosen are $\Omega_1=3\gamma$, $\Omega_2=5\gamma$, $\delta=0$, $\Delta_1=0$, $\Delta_2=2\gamma$, $r_{12}=0.1\lambda$, and $\phi=\pi/4$. The solid line corresponds to $\theta=\pi/2$, the dashed line is for $\theta=0$. (a) Short-time evolution, (b) long-time limit. The oscillatory behavior of the intensity for $\theta=\pi/2$ remains undamped in the long-time limit.

Our main observable is the total fluorescence intensity I_y given in Eq. (19).

Figure 2 shows the intensity I_y for $\Omega_1=3\gamma$, $\Omega_2=5\gamma$, $\delta=0$, $\Delta_1=0$, $\Delta_2=2\gamma$, $r_{12}=0.1\lambda$, $\phi=\pi/4$, and for two different values of θ: $\theta=0,\pi/2$. It can be seen that after an initial phase of rapid changes in the intensity, the sample comes to a time-independent steady state for $\theta=0$, whereas it undergoes periodic changes for $\theta=\pi/2$. These changes persist undamped in the dynamics, as can be seen in Fig. 2(b), which shows the intensity for same parameters as in Fig. 2(a), but for times $t>1000\gamma^{-1}$.

The interpretation of this effect is straightforward: For $\theta=0$, the dipole-dipole cross-couplings Γ_{vc}^{dd} and Ω_{vc}^{dd} are zero. Thus the coefficients on the right hand side of the master equation (6) are time independent, and the system approaches a time-independent steady state. For $\theta=\pi/2$, the dipole-dipole cross couplings Γ_{vc}^{dd} and Ω_{vc}^{dd} are nonzero, and induce an explicit time-dependence in the master equation coefficients, which accounts for the nonstationary long time behavior. This effect is somewhat similar to a two-level system driven by a bichromatic field. Also in this case, the long-time limit is nonstationary. In our system under conditions where the dipole-dipole cross couplings are nonzero, each transition is driven both by a laser field and by the cross coupling contribution. In general, these two contributions have different detunings, and thus induce the nonstationary behavior. This interpretation can easily be verified.

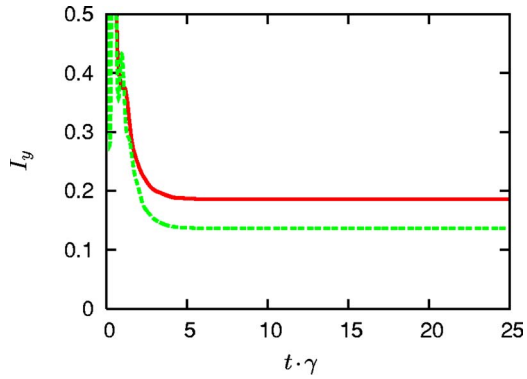

FIG. 3. (Color online) Same as in Fig. 2, but with $\delta=-2\gamma$ and thus $\Delta=0$. In this case, both for $\theta=0$ and $\theta=\pi/2$, the long-time limit intensity is time independent.

The interaction picture in Eq. (6) is chosen such that the only time dependence that may occur is $\exp(\pm i\Delta t)$, where $\Delta=\delta+\Delta_2-\Delta_1$ is a combination of the laser field detunings and the frequency difference of the two lower states. If the nonstationary behavior is due to this time dependence, then the system should approach a constant steady state for any geometry if $\Delta=0$. This is indeed the case, as can be seen in Fig. 3. Here, the same parameters as in Fig. 2 are shown except for $\delta=-2\gamma$, such that $\Delta=0$. Both for $\theta=0$ and $\theta=\pi/2$, the system approaches a true steady state. Note that one may also rewrite the frequency of the time dependence as $\Delta=\nu_2-\nu_1$, i.e., the difference of the two driving field frequencies. This further substantiates the interpretation along the lines of a bichromatic driving of each of the atomic transitions.

Next we study the dependence of the long-time limit on the angle ϕ. For this, we take parameters as in Fig. 2 with $\theta=\pi/2$ and $\phi=0,0.1\pi,0.25\pi,0.4\pi,0.5\pi$. The result is shown in Fig. 4. It can be seen that the angle ϕ modifies the depth of the intensity modulations. For $\phi=0$ and $\phi=0.5\pi$, there are no modulations, as then the dipole-dipole cross coupling vanishes. The maximum modulation occurs for $\phi=0.25\pi$, intermediate modulations are obtained for $\phi=0.1\phi$ and $\phi=0.4\pi$.

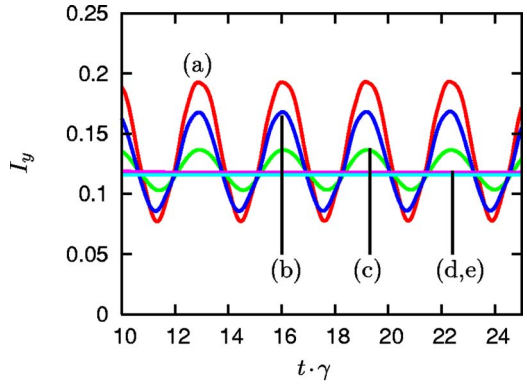

FIG. 4. (Color online) Dependence of the modulation of the fluorescence in the long-time limit on the angle ϕ. (a) $\phi=0.25\pi$, (b) $\phi=0.1\pi$, (c) $\phi=0.4\pi$, (d) $\phi=0$, (e) $\phi=0.5\pi$. The other parameters are as in Fig. 2 with $\theta=\pi/2$.

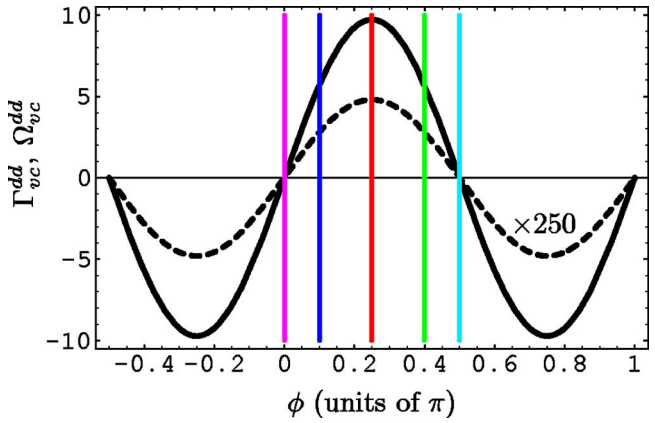

FIG. 5. (Color online) Dependence of the vacuum-induced coupling constants Γ_{vc}^{dd} and Ω_{vc}^{dd} on the angle ϕ. The parameters are as in Fig. 4. The solid curve shows Ω_{vc}^{dd}, the dashed curve is for $250\times\Gamma_{vc}^{dd}$. The vertical lines indicate the phase values shown in Fig. 4.

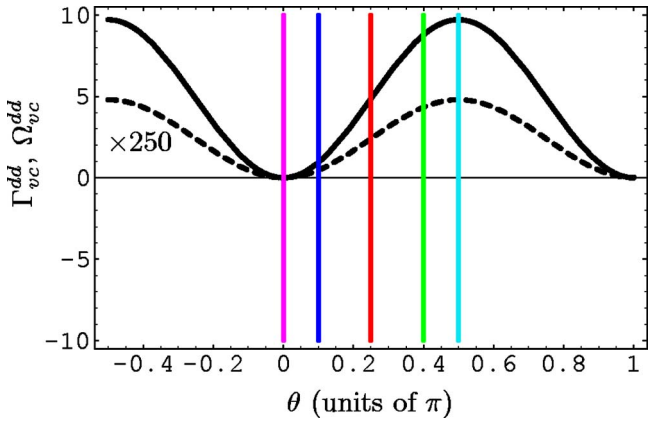

FIG. 7. (Color online) Dependence of the vacuum-induced coupling constants Γ_{vc}^{dd} and Ω_{vc}^{dd} on the angle θ. The parameters are as in Fig. 6. The solid curve shows Ω_{vc}^{dd}, the dashed curve is for $250\times\Gamma_{vc}^{dd}$. The vertical lines indicate the phase values shown in Fig. 6.

The dependence on ϕ can be understood by looking at the ϕ-dependence of the vacuum-induced coupling constants Γ_{vc}^{dd} and Ω_{vc}^{dd}, see Fig. 5. The total fluorescence intensity has a time independent long-time behavior for phase values where the coupling constants vanish. For maximum coupling constants, the intensity modulation is maximum. The modulation amplitude cannot, however, be understood in terms of the coupling constants only. For $\phi=0.1\pi$ and $\phi=0.4\pi$, the coupling constants have identical values, while the fluorescence intensity has different modulation amplitudes. The reason for this is that the angle ϕ also enters the fluorescence intensity via the exponential of the cross terms in Eq. (19), where the two ϕ values yield different results.

The dependence on θ is shown in Fig. 6, with the dependence of the corresponding vacuum-induced couplings in Fig. 7. As for the angle ϕ, the modulation vanishes for vanishing couplings Γ_{vc}^{dd} and Ω_{vc}^{dd}. The interpretation in terms of the magnitude of the coupling constants, however, is difficult as a change of θ also has impact on other variables. This arises mainly from the fact that θ determines the relative position of the two atoms with respect to the laser propagation direction, such that the Rabi frequencies Ω_j depend on θ.

The study of the influence of the various detunings is somewhat complicated by the fact that for equal detunings of the driving fields, the system moves into a dark state due to coherent population trapping, such that the intensity is zero. Thus in Fig. 8, we show the dependence of the intensity long-time limit modulation on the lower-level splitting δ for $\Delta_2=-\Delta_1=\gamma$. Thus one has $\Delta=\delta+2\gamma$, and it is not surprising that the frequency of the modulation decreases with decreasing δ until there is no modulation for $\delta=-2\gamma$.

IV. PHYSICAL INTERPRETATION OF THE NEW COHERENCES

In this section we investigate the physical origin of the cross-coupling terms Γ_{vc}^{dd} and Ω_{vc}^{dd} that arise from the interaction between a dipole of one of the atoms and the *perpendicular* dipole of the other atom. In general, vacuum-mediated interactions arise from an emission of a virtual photon on one transition and the absorption of the photon on

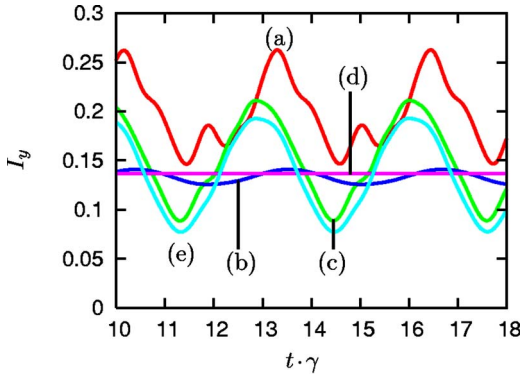

FIG. 6. (Color online) Dependence of the modulation of the fluorescence in the long-time limit on the angle θ. (a) $\theta=0.25\pi$, (b) $\theta=0.1\pi$, (c) $\theta=0.4\pi$, (d) $\theta=0$, (e) $\theta=0.5\pi$. The other parameters are as in Fig. 2 with $\phi=\pi/4$.

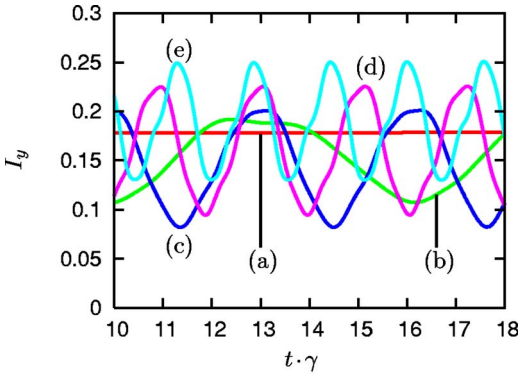

FIG. 8. (Color online) Dependence of the modulation of the fluorescence in the long-time limit on the lower-state splitting δ. Parameters are as in Fig. 2 with $\theta=\pi/2$, but with $\Delta_1=-\gamma$ and $\Delta_2=\gamma$. (a) $\delta=-2\gamma$, (b) $\delta=-\gamma$, (c) $\delta=0$, (d) $\delta=\gamma$, (e) $\delta=2\gamma$.

the same or another transition. In a single atom, such interactions where the absorbing and the emitting transition are the same lead to the complex Lamb shift. Any dipole-dipole interaction between different dipole moments, however, for a single atom in plain vacuum strictly requires the dipoles to be nonorthogonal. This is clearly the case since the dipole moments must couple to a common set of modes.

In contrast, in the present case of two atoms separated by a distance r_{12}, the cross coupling terms Γ_{vc}^{dd} and Ω_{vc}^{dd} can be different from zero although the two involved dipole moments are orthogonal. As in a single atom, a coupling between dipole moments of different atoms is only possible if the involved transitions couple to a common set of modes, i.e., photons emitted by one transition can be absorbed on a transition of the other atom. Here we illustrate why this condition can be fulfilled even between orthogonal dipole moments belonging to different atoms. For this, we return to the equation of motion (16) for the field modes $a_{k\lambda}$ and keep only the source contribution from the transition $1 \leftrightarrow 3$ of atom 1. The corresponding electric field operator then reads

$$\boldsymbol{E}_{\boldsymbol{d}_1}^{(1)}(\boldsymbol{x},t) = \frac{i}{\hbar}\sum_{k\lambda} \boldsymbol{u}_{k\lambda}(\boldsymbol{x}) \int_0^t e^{-i\omega_k \tau}[\boldsymbol{d}_1 \cdot \boldsymbol{u}_{k\lambda}(\boldsymbol{r}_1)^*] \tag{20}$$

$$[S_{13}^{(1)}(t-\tau) + S_{31}^{(1)}(t-\tau)]d\tau + \text{H.c.},$$

where we again assumed that the dipole moment $\boldsymbol{d}_1$ is real. The aim is to evaluate Eq. (20) at the position $\boldsymbol{r}_2$ of atom 2. In contrast to the derivation of Eq. (17), the calculation has to be performed without taking the far field limit since the atoms are close to each other. We follow the steps outlined in Chap. 8 of Ref. [3] and obtain

$$\boldsymbol{E}_{\boldsymbol{d}_1}^{(1)}(\boldsymbol{r}_2,t) = S_{13}^{(1)}(t)\vec{\vec{\chi}}(\boldsymbol{r}_1,\boldsymbol{r}_2)\cdot\boldsymbol{d}_1 + \text{H.c.} \tag{21}$$

$$= S_{13}^{(1)}(t)\left[f_1(k_0,r_{12})\boldsymbol{d}_1 - f_2(k_0,r_{12})\frac{(\boldsymbol{d}_1\cdot\boldsymbol{r}_{12})\boldsymbol{r}_{12}}{r_{12}^2}\right] + \text{H.c.} \tag{22}$$

The definitions of the functions f_1, f_2 follow directly from Eqs. (12) and (21) and will not be given here. $\boldsymbol{E}_{\boldsymbol{d}_1}^{(1)}(\boldsymbol{r}_2,t)$ can be regarded as the field radiated by the dipole $\boldsymbol{d}_1$ of atom 1 at the position of atom 2. Note that a similar expression is obtained in the case of a classical radiating dipole at $\boldsymbol{r}_1$ [30]. Obviously, the polarization of $\boldsymbol{E}_{\boldsymbol{d}_1}^{(1)}(\boldsymbol{r}_2,t)$ depends on the relative orientation of the atoms. In particular, from Eq. (22) it follows that $\boldsymbol{E}_{\boldsymbol{d}_1}^{(1)}(\boldsymbol{r}_2,t)$ contains not only a contribution along $\boldsymbol{d}_1$, but also a term proportional to $\boldsymbol{r}_{12}$. Therefore, a photon emitted by atom 1 on the $1 \leftrightarrow 3$ transition can be absorbed by atom 2 on the $2 \leftrightarrow 3$ transition, provided that the projection of $\boldsymbol{r}_{12}$ onto $\boldsymbol{d}_2$ is different from zero, i.e., $\boldsymbol{r}_{12}\cdot\boldsymbol{d}_2 \neq 0$. The dipole moment $\boldsymbol{d}_1$ of atom 1 can thus be coupled to the orthogonal dipole moment $\boldsymbol{d}_2$ of atom 2 since the field radiated by the former dipole moment may exhibit a component along the latter dipole moment.

In order to verify the consistency of this explanation, we consider the projection of $\boldsymbol{E}_{\boldsymbol{d}_1}^{(1)}(\boldsymbol{r}_2,t)$ onto $\boldsymbol{d}_2$. This expression should exhibit the same dependence on the relative position $\boldsymbol{r}_{12}$ of the two atoms as the cross-coupling terms Γ_{vc}^{dd} and Ω_{vc}^{dd}. In fact, with the help of Eqs. (10), (11), and (21) we arrive at

$$\boldsymbol{d}_2\cdot\boldsymbol{E}_{\boldsymbol{d}_1}^{(1)}(\boldsymbol{r}_2,t) = \hbar\Omega_{vc}^{dd}(S_{13}^{(1)}(t) + S_{31}^{(1)}(t)) + i\hbar\Gamma_{vc}^{dd}(S_{13}^{(1)}(t) - S_{31}^{(1)}(t)). \tag{23}$$

Thus, the real and imaginary parts of $\boldsymbol{d}_2\cdot\boldsymbol{E}_{\boldsymbol{d}_1}^{(1)}(\boldsymbol{r}_2,t)$ show indeed the same dependence on r_{12}, θ, and ϕ as the coupling coefficients Ω_{vc}^{dd} and Γ_{vc}^{dd}, respectively.

From another point of view, the preceding discussion shows that for certain relative positions of the atoms each dipole of atom 2 interacts with both dipoles of atom 1 and vice versa. We finally perform a thought experiment and replace atom 2 by a photodetector with a polarization filter in front of it. The question is now if this detector is able to discriminate between photons that stem from dipole moments $\boldsymbol{d}_1$ and $\boldsymbol{d}_2$ of atom 1. Surprisingly, the answer is no since the fields radiated by $\boldsymbol{d}_1$ and $\boldsymbol{d}_2$ are never orthogonal to each other at any position where Γ_{vc}^{dd} and Ω_{vc}^{dd} are different from zero. In this sense, the orthogonal dipole moments of different atoms are forced to interact, since the absorbing atom cannot distinguish between photons originating from the two transitions of the emitting atom.

V. DISCUSSION AND SUMMARY

In the previous Sec. IV, we have shown that the peculiar vacuum-induced coupling of orthogonal transition dipole moments can be understood in terms of the dipole radiation pattern. For certain geometries, the field emitted by one transition of the first atom has components parallel to each of the transition dipole moments of the second atom, even if the emitting and absorbing dipoles are orthogonal. Thus the second atom cannot decide on which transition the photon was emitted by the first atom.

Speaking generally, this result is of relevance for experimental realizations of collective few-level systems. For example, in real atoms, usually additional transitions are present, e.g., from the ground state to other Zeeman sublevels of the excited state. Then it may not be possible to realize, e.g., a pure two-level system by choosing the polarization of the driving fields appropriately, as the vacuum-induced coupling of orthogonal dipole moments can populate unwanted extra energy levels.

The collective effects in samples of atoms arise from vacuum-induced dipole-dipole couplings between transitions in different atoms. These couplings are analogous to virtual interactions of a single transition and the vacuum, which gives rise to the complex Lamb shift, and to virtual interactions between different transitions in a single atom, responsible for spontaneously generated coherences. The coupling of orthogonal dipole moments by virtual photons discussed here, however, is not possible in single atoms interacting with the plain isotropic vacuum. Therefore the vacuum-coupling of orthogonal dipole moments observed here is a collective effect.

In summary, we have discussed the dynamics of a pair of nearby three-level systems in Λ configuration. We have shown that in contrast to the single-atom case, transitions in

the two atoms can be dipole-dipole coupled via the vacuum field even if the transition dipole moments are orthogonal. This additional coupling can strongly affect the system dynamics. For otherwise fixed parameters, the relative position of the two atoms alone can decide whether the system has a stationary steady state or not. As a consequence, the total fluorescence intensity emitted by the composite system is either stationary or "blinks" at a characteristic frequency in the long-time limit, depending on the alignment of the two atoms. The coupling of orthogonal dipole moments occurs if the absorbing atom is unable to distinguish between photons emitted by the two transitions of the other atom.

[1] R. H. Dicke, Phys. Rev. **93**, 99 (1954).
[2] R. H. Lehmberg, Phys. Rev. A **2**, 883 (1970).
[3] G. S. Agarwal, in *Quantum Statistical Theories of Spontaneous Emission and Their Relation to Other Approaches*, edited by G. Hohler (Springer, Berlin, 1974).
[4] Z. Ficek and S. Swain, *Quantum Interference and Coherence: Theory and Experiments* (Springer, Berlin, 2005).
[5] M. Gross and S. Haroche, Phys. Rep. **93**, 301 (1982).
[6] M. Macovei, J. Evers, and C. H. Keitel, Phys. Rev. Lett. **91**, 233601 (2003).
[7] S. S. Hassan, G. P. Hildred, R. R. Puri, and R. K. Bullough, J. Phys. B **15**, 2635 (1982).
[8] P. D. Drummond and H. J. Carmichael, Opt. Commun. **27**, 160 (1978); S. Y. Kilin, Sov. Phys. JETP **55**, 38 (1982).
[9] M. Macovei, J. Evers, and C. H. Keitel, Europhys. Lett. **68**, 391 (2004).
[10] M. A. Macovei and J. Evers, Opt. Commun. **240**, 379 (2004).
[11] N. N. Bogolubov, Jr., T. Quang, and A. S. Shumovsky, Phys. Lett. **112**, 323 (1985).
[12] J. M. Raimond, P. Goy, M. Gross, C. Fabre, and S. Haroche, Phys. Rev. Lett. **49**, 117 (1982).
[13] T. J. Carroll, K. Claringbould, A. Goodsell, M. J. Lim, and M. W. Noel, Phys. Rev. Lett. **93**, 153001 (2004).
[14] M. Macovei and C. H. Keitel, Phys. Rev. Lett. **91**, 123601 (2003).
[15] T. G. Rudolph, Z. Ficek, and B. J. Dalton, Phys. Rev. A **52**, 636 (1995).
[16] D. F. V. James, Phys. Rev. A **47**, 1336 (1993).
[17] M. Lewenstein and J. Javanainen, Phys. Rev. Lett. **59**, 1289 (1987); A. Beige and G. C. Hegerfeldt, Phys. Rev. A **59**, 2385 (1999).
[18] G. V. Varada and G. S. Agarwal, Phys. Rev. A **45**, 6721 (1992).
[19] M. D. Lukin, and P. R. Hemmer, Phys. Rev. Lett. **84**, 2818 (2000); G.-x. Li, K. Allaart, and D. Lenstra, Phys. Rev. A **69**, 055802 (2004).
[20] I. V. Bargatin, B. A. Grishanin, and V. N. Zadkov, Phys. Rev. A **61**, 052305 (2000).
[21] R. G. DeVoe, and R. G. Brewer, Phys. Rev. Lett. **76**, 2049 (1996); P. Mataloni, E. DeAngelis, and F. DeMartini, *ibid.* **85**, 1420 (2000); J. Eschner, C. Raab, F. Schmidt-Kaler, and R. Blatt, Nature (London) **413**, 495 (2001); M. D. Barnes, P. S. Krstic, P. Kumar, A. Mehta, and J. C. Wells, Phys. Rev. B **71**, 241303(R) (2005).
[22] Z. Ficek and R. Tanas, Phys. Rep. **372**, 369 (2002).
[23] Z. Ficek, Phys. Rev. A **44**, 7759 (1991).
[24] G. S. Agarwal and A. K. Patnaik, Phys. Rev. A **63**, 043805 (2001).
[25] M. O. Scully and M. S. Zubairy, *Quantum Optics* (Cambridge University Press, Cambridge, 1997).
[26] S. Y. Zhu and M. O. Scully, Phys. Rev. Lett. **76**, 388 (1996); P. Zhou and S. Swain, *ibid.* **77**, 3995 (1996); S. Y. Zhu, L. M. Narducci, and M. O. Scully, Phys. Rev. A **52**, 4791 (1995); H. Huang, S. Y. Zhu, and M. S. Zubairy, *ibid.* **55**, 744 (1997); E. Paspalakis and P. L. Knight, Phys. Rev. Lett. **81**, 293 (1998); M. O. Scully and S. Y. Zhu, Science **281**, 1973 (1998); C. H. Keitel, Phys. Rev. Lett. **83**, 1307 (1999); E. Frishman and M. Shapiro, *ibid.* **87**, 253001 (2001); G. S. Agarwal, *ibid.* **84**, 5500 (2000); J. Evers, D. Bullock, and C. H. Keitel, Opt. Commun. **209**, 173 (2002); U. Akram and Z. Ficek, J. Opt. Soc. Am. B **5**, 330 (2003).
[27] J. Evers and C. H. Keitel, J. Phys. B **37**, 2771 (2004); Z. Ficek and S. Swain, Phys. Rev. A **69**, 023401 (2004).
[28] H. R. Xia, C. Y. Ye, and S. Y. Zhu, Phys. Rev. Lett. **77**, 1032 (1996); L. Li, X. Wang, J. Yang, G. Lazarov, J. Qi, and A. M. Lyyra, *ibid.* **84**, 4016 (2000).
[29] P. W. Milonni and P. L. Knight, Phys. Rev. A **10**, 1096 (1974).
[30] See, for example, Chap. 2.2.3 in M. Born and E. Wolf, *Principles of Optics* (Cambridge University Press, Cambridge, 1999).